Results in Engineering 30 (2026) 110605

Contents lists available at ScienceDirect

Results in Engineering

journal homepage: www.sciencedirect.com/journal/results-in-engineering

Crashworthiness performance of pentagonal multi-cell carbon filament/aluminium circular hybrid tube under axial crushing

Willy Artha Wirawan [a,*], Delia Hani Wakhidah [a], Diah Wulandari [a], A'yan Sabitah [b], Moch. Agus Choiron [c], Joewono Prasetijo [d,e], S.M. Sapuan [f]

[a] Applied Mechanical Engineering Study Program, Faculty of Vocational Studies, Universitas Negeri Surabaya, Jl. Ketintang, Surabaya 60231, Indonesia
[b] Mechanical Engineering Department, Politeknik Negeri Banjarmasin, Jl. Brig Jend. Hasan Basri, Kalimantan 70124, Indonesia
[c] Mechanical Engineering Department, Brawijaya University, Mayjen Haryono Street 165 Malang 65145, Indonesia
[d] Faculty of Civil Engineering and Planning, Universitas Internasional Batam, Batam, 29426, Indonesia
[e] Universiti Tun Hussein Onn Malaysia, Parit Raja, Batu Pahat, Johor Darul Ta'zim 86400, Malaysia
[f] Advanced Engineering Materials and Composites Research Centre (AEMC), Department of Mechanical and Manufacturing Engineering, Universiti Putra Malaysia, 43400 UPM Serdang, Selangor, Malaysia

ARTICLE INFO

Keywords:
3D printing
Hybrid tube
Pentagonal
Multi-cell
Quasi static
Crashworthiness

ABSTRACT

The main objective of this study was to evaluate the energy absorption capability and impact deformation behavior of an additional reinforcement in a hybrid carbon-filament structure as an optimal impact-resistant configuration. The hybrid tubes were fabricated using aluminum and carbon fiber 3D-printing filaments, with a pentagonal geometry applied to the inner sidewall. Four pentagonal-dimensional models were developed and categorized as Very Small Range (HPVS), Small Range (HPSR), Medium Range (HPMR), and Large Range (HPLR). Quasi-static compression tests were conducted experimentally to characterize the structural behavior of the hybrid tube configurations under quasi-static. The results showed that the HPSR model exhibited the highest energy absorption, reaching 3.522 kJ, followed by HPMR with 3.067 kJ, HPLR with 3.050 kJ, and HPVS with 2.844 kJ. The load-displacement curves revealed a consistent and distinct deformation pattern within the displacement range of 0-65 mm for all models. In contrast, within the displacement range of 65-100 mm, the HPLR and HPVS models exhibited irregular responses, indicating buckling phenomena that compromised structural stability and integrity. Overall, the hybrid pentagonal design offers a well-balanced solution in terms of energy absorption (EA), specific energy absorption (SEA), crush force efficiency (CFE), and peak crushing force (PCF), indicating its strong potential for application in future energy-absorbing structures.

1. Introduction

Crashworthy structures are increasingly required in automotive, railway, and aerospace systems to mitigate transmitted loads during impact while maintaining lightweight design. Thin-walled tubes remain among the most widely used energy absorbers because they can dissipate impact energy through progressive plastic deformation under axial loading. However, conventional single-material tubes often involve a trade-off among mass efficiency, peak crushing force, and deformation stability, particularly when local buckling develops prematurely. This limitation has motivated the development of hybrid crashworthy structures that combine materials with complementary mechanical characteristics to enhance energy absorption while preserving structural integrity [1–6].

Recent studies have shown that crashworthiness is governed not only by material selection but also by internal architecture. Hybrid metal-composite tubes, multi-cell sections, foam-filled tubes, and origami-inspired designs can improve crushing stability by increasing the number of load paths and controlling fold formation during collapse [7–12]. In parallel, three-dimensional printing technologies have enabled the fabrication of complex cellular reinforcements that are difficult to produce using conventional methods, thereby allowing internal geometries to be tailored for specific deformation responses under quasi-static and impact loading [13–17]. These developments indicate that the geometric design of the internal structure has become a primary variable in crashworthy design and is often as important as the base material system

* Corresponding authors.
E-mail address: willywirawan@unesa.ac.id (W.A. Wirawan).

https://doi.org/10.1016/j.rineng.2026.110605
Received 13 April 2026; Accepted 17 April 2026
Available online 19 April 2026

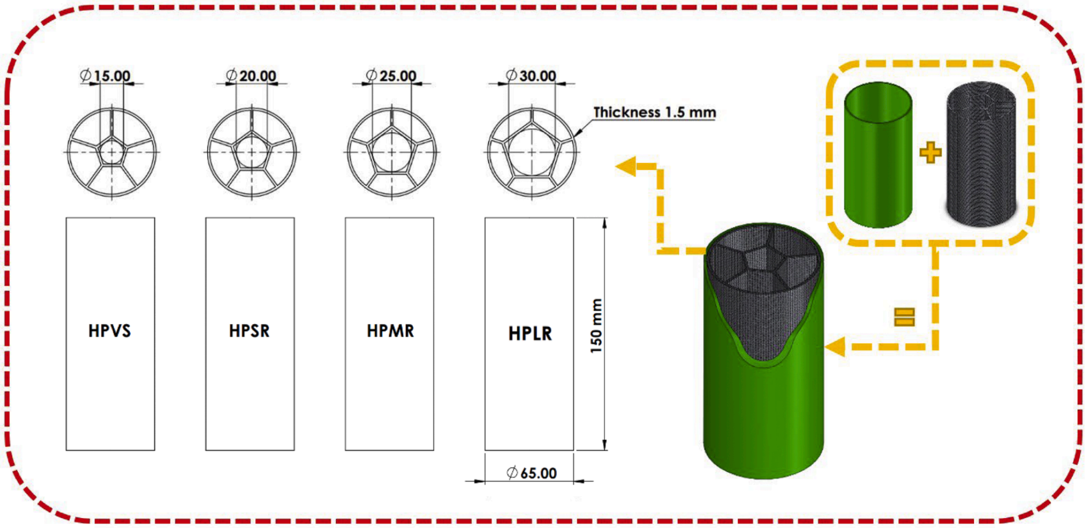

Fig. 1. Geometries of the pentagonal multi-cell hybrid tube models: (a) HPVS, (b) HPSR, (c) HPMR, and (d) HPLR.

itself.

This geometry-driven trend is also evident in recent studies on metamaterials and hierarchical cellular absorbers. A recent review by Cai and Deng [18] showed that reinforced honeycomb mechanical metamaterials can achieve substantial improvements in stiffness, load transfer, and energy dissipation through architecture-based reinforcement rather than material substitution alone. In a related study, Cai and Deng [19]. demonstrated that novel hybrid honeycombs can enhance specific energy absorption by combining distinct cell topologies and symmetry strategies under axial crushing. Likewise, Xu et al. [20]. reported that two-way gradient octagonal hierarchical honeycombs exhibit excellent energy absorption and crashworthiness by integrating hierarchy and geometric grading into the cellular layout. Collectively, these studies highlight a clear research direction: structural topology and geometric proportion strongly influence crushing-mode transition, energy dissipation, and force regulation, and should therefore be treated as key design parameters rather than as secondary geometric details.

Despite this progress, the literature has focused predominantly on square, hexagonal, auxetic, honeycomb, and hierarchical cellular systems, whereas pentagonal internal architectures in hybrid thin-walled tubes remain far less explored. This gap is important because a pentagonal configuration may provide a useful compromise among stiffness, confinement, and progressive folding, particularly when integrated with a circular metallic outer shell. Previous studies on fractal and gradient multi-cell tubes have shown that internal topology can improve specific energy absorption and crush force efficiency by stabilizing deformation and distributing stresses more uniformly along the crushing axis [21–24]. However, these studies mainly addressed hierarchical or non-pentagonal configurations and did not clarify how the relative internal geometry of a pentagonal insert affects the crushing response of a metal-polymer hybrid tube. In particular, the effect of internal pentagonal spacing, or more fundamentally the geometric proportion between the inner pentagonal insert and the outer circular tube, has not been systematically established.

The present study addresses this gap by investigating the crashworthiness of circular aluminum tubes reinforced with three-dimensional-printed carbon-filament pentagonal multi-cell inserts under quasi-static axial crushing. Four configurations were examined, namely Hybrid Pentagonal Very Small Range (HPVS), Hybrid Pentagonal Small Range (HPSR), Hybrid Pentagonal Medium Range (HPMR), and Hybrid Pentagonal Large Range (HPLR), representing different levels of internal geometric spacing within the same hybrid concept. Unlike previous studies that focused mainly on material substitution or non-pentagonal cellular topologies, this work examines how the relative internal pentagonal geometry influences the load-displacement response, deformation mode, and key crashworthiness indicators. The working premise is that the crushing response is governed not by absolute inner size alone, but by the geometric proportion between the internal pentagonal reinforcement and the outer tube. By identifying the configuration that best balances energy absorption and deformation stability, this study contributes to the design of lightweight hybrid energy absorbers for safety-critical structures.

2. Materials and methods

2.1. Geometry and tube design

Hybrid multi-cell structural designs have been reported to enhance crashworthiness behavior and increase the amount of absorbed energy [25–27]. The combined hybrid effect and pentagonal inner-side geometry are expected to suppress buckling phenomena, reduce the initial peak force (IPFC), and improve the specific energy absorption (SEA). Accordingly, a hybrid configuration consisting of circular aluminum tubes and 3D-printed carbon filament inserts was further investigated in this study. To ensure successful specimen fabrication, the outer dimensions of the aluminum tube were designed with a constant cross-sectional inertia, including a length (l) of 150 mm, an outer diameter (d) of 65 mm, a wall thickness (t) of 1.5 mm, and a chamfer angle at the tube end (φ) of 45°. The inner section of the tube was designed as a pentagonal multi-cell structure with the same tube length and diameter, fabricated from 3D-printed carbon filament material. The detailed dimensions of each crashworthiness specimen developed in this study are shown in Fig. 1. The aluminum tube and carbon filament insert were then combined and assembled into a single segment using an interference-fit method [28].

As shown in Fig. 1, the energy absorption performance of pentagonal multi-cell carbon filament/aluminum circular hybrid crashworthiness tubes was investigated using four specimen models:

Model I: HPVS (Hybrid Pentagonal Very Small Range), which represents a very small spacing difference between the outer and inner pentagonal sections.

Model II: HPSR (Hybrid Pentagonal Small Range), which represents a narrow spacing difference, characterized by a small gap between the outer and inner pentagonal sections.

Model III: HPMR (Hybrid Pentagonal Medium Range), which represents an intermediate spacing difference between the narrow and wide

Fig. 2. Fabrication process of the pentagonal multi-cell carbon filament/aluminium hybrid energy-absorbing tube.

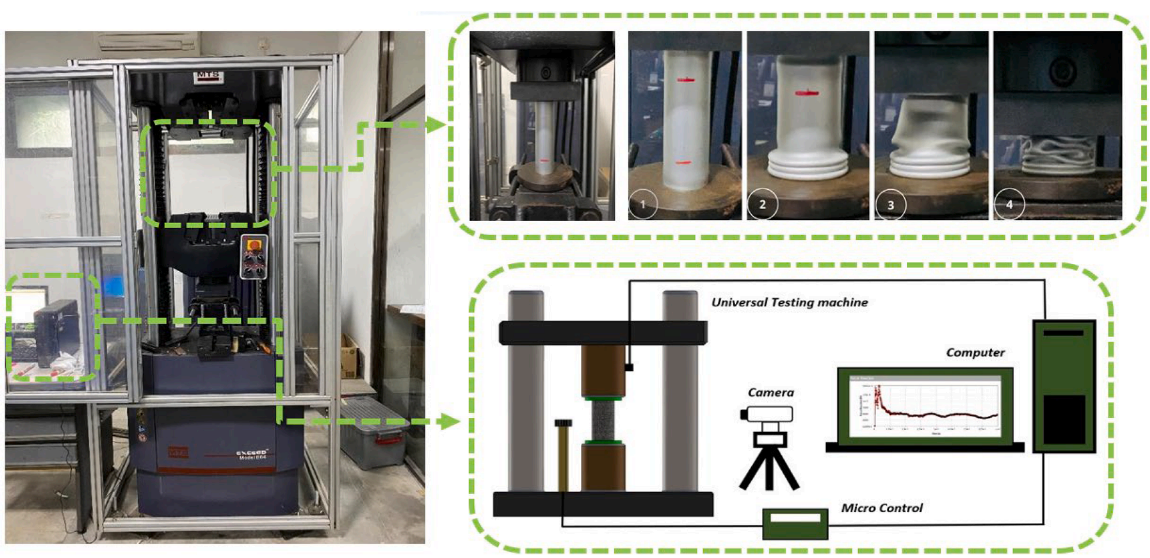

Fig. 3. Schematic of the quasi-static axial crushing test setup.

configurations.

Model IV: HPLR (Hybrid Pentagonal Large Range), which represents a very large spacing difference between the two pentagonal sections, with a significant and clearly visible gap.

2.2. Energy-absorbing tube production

In this study, the crashworthiness structure was fabricated by combining aluminum as the outer material and carbon filament as the inner material (Fig. 2). Aluminum alloy AL 6063-T5 was selected due to its high structural strength and energy absorption capability under crash conditions [29,30]. The inner structure was produced using additive manufacturing with carbon filament. In 3D printing, material is deposited layer by layer according to a geometry generated from CAD software. In the present work, the Fused Deposition Modeling (FDM) process was performed using a RAISE3D PRO2 Plus machine (N2 Plus, Costa Mesa, USA) and carbon fiber filament with a diameter of 1.75 mm. The carbon filament was extruded through the nozzle at a melting temperature of 250 °C, a printing speed of 50 mm/s, and a build-platform temperature of 50 °C [31].

2.3. Quasi-static - axial crushing test experiments

In this study, quasi-static crushing experiments were performed using a SHIMADZU 300 kN Universal Testing Machine (UTM), Japan. The quasi-static test was carried out by placing the specimen on the fixed support of the testing machine, while a rigid impactor compressed the tube at a constant speed of 2 mm/s, as illustrated in Fig. 3. During the crushing process, the displacement was controlled to 75% of the tube height, equivalent to approximately 100 mm. The reaction force and displacement were continuously recorded by the testing machine throughout the test. In addition, the mechanical fracture behavior was documented using a Canon PowerShot SX430 IS digital camera.

2.4. Crashworthiness performance

Several common criteria for evaluating crashworthiness include EA (Energy Absorption), IPFC (Initial Peak Force), SEA (Specific Energy

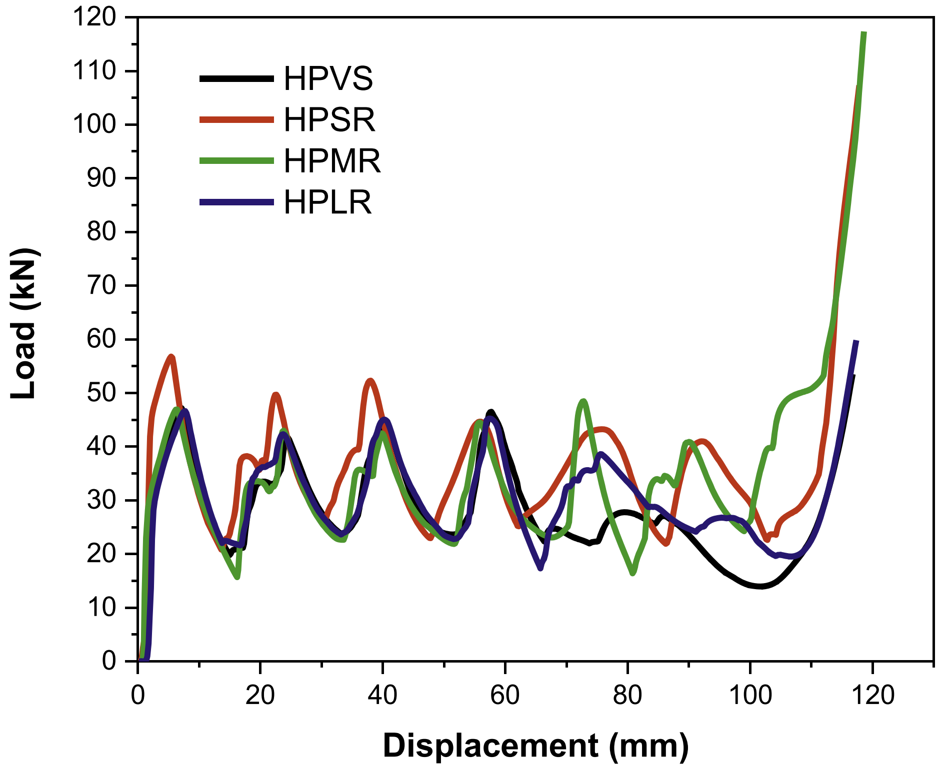

Fig. 4. Load-displacement responses of the pentagonal hybrid tubes.

Absorption), MF (Mean Force), and CFE (Crush Force Efficiency) [32]. Energy absorption (EA) refers to the total energy absorbed during the crushing process and can be determined from the area under the load-displacement curve. Here, F(δ) denotes the crushing force, while δ denotes the crushing displacement obtained from the load-displacement response.

$$EA = \int_0^d f(\delta)d\delta$$

MF (Mean Force) is the average crushing force that reflects the stability of the energy absorption process and can be expressed by the following mathematical equation:

$$MF = \frac{1}{d}\int_0^d f(\delta)d\delta$$

CFE (Crush Force Efficiency) is defined as the ratio of the mean force (MF) to the initial peak force (IPFC), and it is used to indicate the efficiency of the crushing process.

$$\text{CFE} \ = \frac{MF}{IPFC} x \ 100$$

SEA (Specific Energy Absorption) is defined as the amount of energy absorbed per unit mass and can be determined using the following mathematical equation:

$$\text{SEA} = \frac{EA}{m}$$

3. Result and discussion

3.1. Response of crushing

In the quasi-static axial crushing experiments, the load-displacement responses of the four hybrid tube models HPVS, HPSR, HPMR, and HPLR exhibited significant differences in energy absorption characteristics and deformation behavior. Fig. 4 presents the relationship between load (kN) and displacement (mm) for each configuration of the pentagonal multi-cell carbon filament/aluminum circular hybrid tube design.

Fig. 4. presents the relationship between load and displacement obtained from the quasi-static axial crushing tests. The curve patterns exhibit distinct characteristics and stages that correspond to the material response under applied loading. The results of the axial crushing tests reveal significant differences in the crashworthiness performance among the four models.

The HPSR model (Hybrid Pentagonal Small Range) demonstrates the most stable and consistent response throughout the experiment, with load fluctuations ranging between 25–55 kN, which are higher than those observed in the other models. In contrast, the HPLR model (Hybrid Pentagonal Large Range) and the HPVS model (Hybrid Pentagonal Very Small Range) exhibit unstable responses within the displacement range of 70–100 mm, indicating the occurrence of buckling phenomena that compromise structural integrity. Meanwhile, the HPMR model (Hybrid Pentagonal Medium Range) shows a relatively stable increase in load, although its performance is not as optimal as that of the HPSR model.

Overall, the HPSR model demonstrates the best performance in terms of energy absorption capability and deformation stability, exhibiting more controlled characteristics throughout the crushing process. In addition, a unique phenomenon is observed at the end of the load–displacement curves, where the HPMR and HPSR models are able to sustain a final peak load of up to 110 kN. This behavior is particularly important in collision scenarios, where the tube can absorb a substantial amount of energy after undergoing stable deformation while maintaining a relatively low initial peak crushing force (IPFC).

A similar mechanism has been reported in corrugated thin-walled tube designs, where the fracture phenomenon is conditioned in such a way that the tube is capable of absorbing impact energy with lower risk. This occurs because the initial peak crushing force (IPFC) at the early stage of impact remains relatively low while maintaining optimal values of crush force efficiency (CFE) and specific energy absorption (SEA) [33,

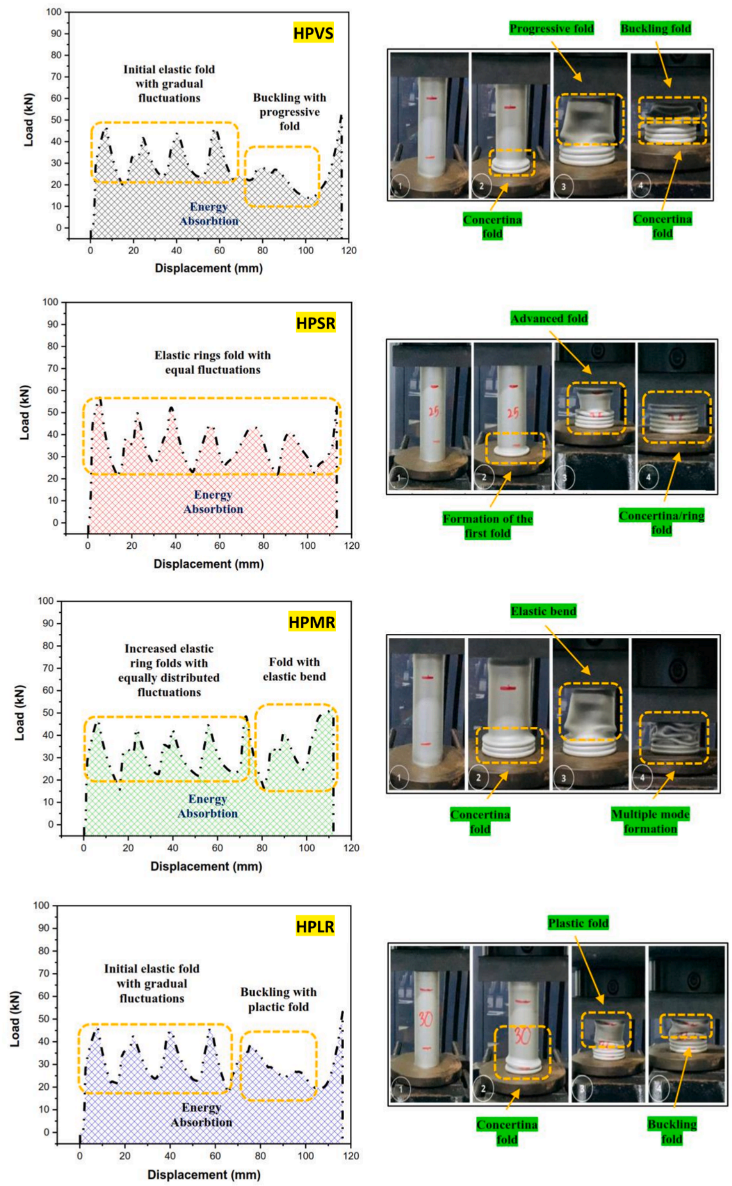

Fig. 5. Energy absorption characteristics and deformation modes of the pentagonal hybrid tube.

34].

As shown in Fig. 5, the Energy Absorption (EA) capacity of the four hybrid tube configurations HPVS, HPSR, HPMR, and HPLR exhibits significant differences. Quantitatively, the HPSR model shows the highest EA value of 3.522 kJ, followed by HPMR with 3.067 kJ, HPLR with 3.050 kJ, and HPVS with 2.844 kJ. These results indicate that the HPSR configuration is capable of absorbing impact energy more effectively than the other models. The results of the axial crushing tests on the pentagonal multi-cell hybrid tubes also reveal a strong correlation between the load–displacement curves and the deformation patterns observed in each model. The HPSR model (Hybrid Pentagonal Small Range) exhibits the most stable load response, characterized by uniform fluctuations throughout the displacement range up to 120 mm. This behavior is consistent with the formation of elastic ring folds with equal fluctuations and concertina/ring folds observed in the deformation pattern. Such behavior indicates a controlled progressive deformation mechanism and high energy absorption efficiency, allowing the structure to maintain optimal stability during the crushing process. In contrast, the HPVS (Very Small Range) and HPLR (Large Range) models show significant load fluctuations within the displacement range of 70–100 mm. These responses are associated with deformation modes such as buckling with progressive folds and non-uniform concertina folds. The instability observed in the HPLR model is primarily caused by the large difference between the internal and external diameters, which results in uneven internal force distribution. The stiffer regions of the tube tend to trigger localized deformation and the formation of local cracks, thereby reducing the energy absorption capacity during the intermediate stage of crushing [35,36]. Meanwhile, in the HPVS model, the very small pentagonal size increases stress concentration at the internal corners. As a result, these regions experience earlier bending and localized deformation, which subsequently triggers buckling phenomena [29,37].

The HPMR model (Hybrid Pentagonal Medium Range) exhibits a gradual increase in load with moderate fluctuations, which corresponds to deformation patterns characterized by increased elastic ring folds with equally distributed fluctuations and folds with elastic bending. This behavior indicates a more uniform stress distribution compared with the HPVS and HPLR models, although its performance is still inferior to that of the HPSR model. In this study, it was found that a moderate internal-to-external diameter ratio, as observed in the HPSR configuration,

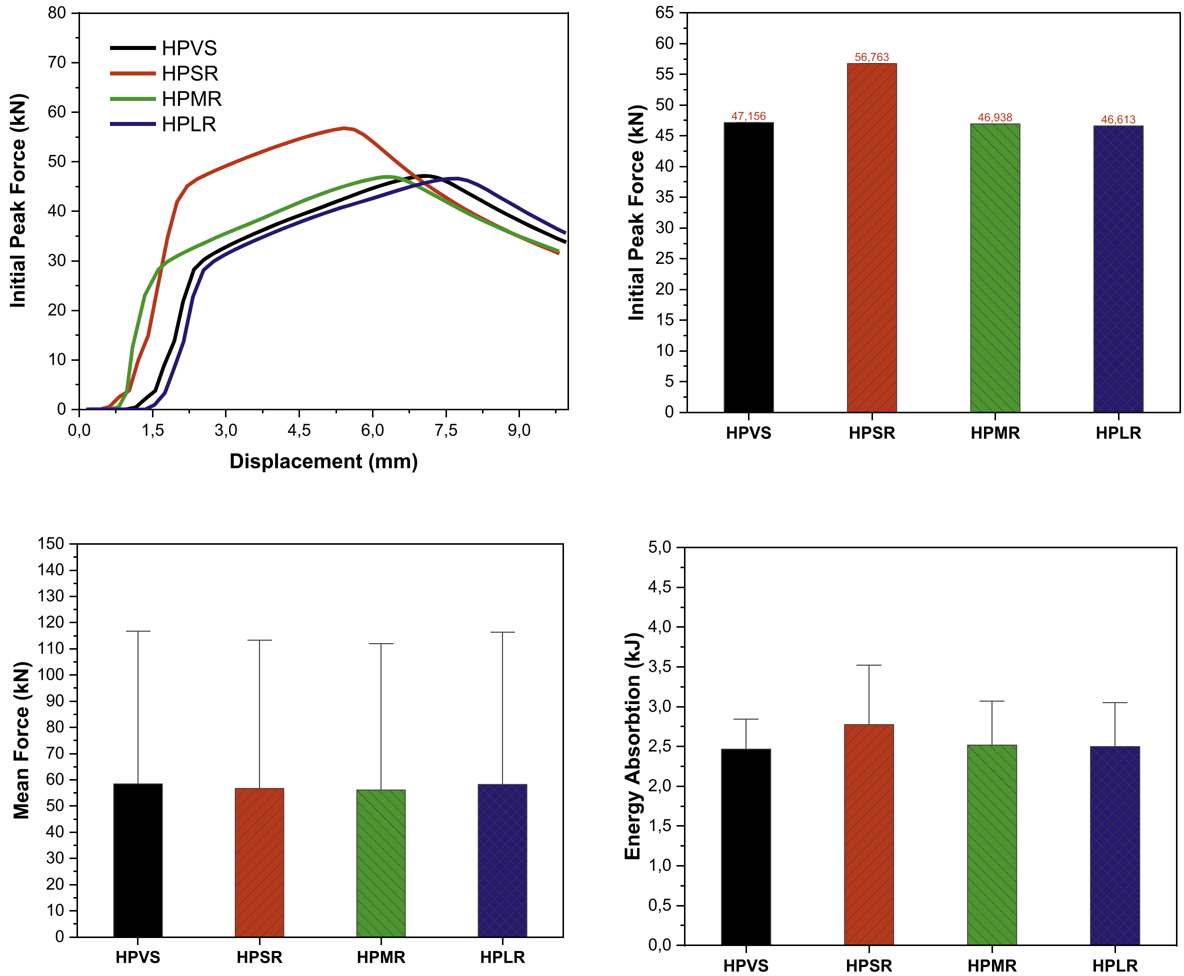

Fig. 6. Comparison of crashworthiness indicators for the pentagonal hybrid tube.

produces a more progressive and stable deformation mode, thereby improving energy absorption efficiency. These findings are consistent with previous studies indicating that the internal geometric configuration of hybrid tubes significantly influences deformation stability and energy absorption performance [38–40]. Therefore, proper control of the internal geometry becomes a key factor in the design of hybrid tubes for crashworthiness applications. In contrast, excessively small or excessively large diameter variations may induce mechanical instability and reduce the overall efficiency of energy absorption.

3.2. *Crashworthiness performance*

The crashworthiness performance analysis of the four hybrid tube configurations HPVS, HPSR, HPMR, and HPLR reveals significant differences in energy absorption capability and initial deformation response, as illustrated by the IPFC curves presented in Fig. 6. The HPSR model exhibits the highest IPFC value of 56.76 kN, indicating a greater structural capacity to withstand the initial load compared with HPVS (47.16 kN), HPMR (46.94 kN), and HPLR (46.61 kN). The HPSR configuration demonstrates the highest IPFC value, representing an increase of approximately 20.2% compared with the HPVS model, while HPMR and HPLR display nearly identical and relatively lower IPFC values. The HPSR model possesses the highest initial load-bearing capacity, which enables superior performance under high-impact conditions. However, it may pose potential risks in low-impact scenarios, where excessively high initial forces are difficult to absorb effectively and may trigger buckling phenomena [33]. In contrast, the HPLR model, with a moderate IPFC value, is recommended for applications involving low- to medium-impact loads. In such cases, the deformation process becomes more progressive and controlled, thereby reducing the risk of premature structural damage.

The increase in IPFC can be attributed to the enhanced stiffness of the tubes resulting from the addition of the pentagonal multi-cell carbon filament structure, which improves the structural resistance to axial loading during the initial displacement stage of 2–4 mm before the onset of major deformation. This phenomenon is consistent with observations in hybrid tubes made of CFRP materials, where fiber reinforcement increases the initial load-bearing capacity as well as the fracture energy of the tube [37,41]. Although the IPFC value of the HPSR configuration is slightly higher, the difference compared with the HPLR and HPMR models is relatively small (<5%). Therefore, in practical terms, all configurations demonstrate adequate capability to withstand the initial load, providing design flexibility for various impact scenarios.

The Mean Force (MF) parameter across all models shows relatively similar values, indicating that after the initial peak phase, all configurations are able to maintain a stable average force during the axial deformation process. This observation is also confirmed by the characteristics of the load–displacement curves, where after the load reaches the IPFC peak, the reduction in force is not significant and the deformation proceeds with a relatively uniform force distribution. This behavior indicates that the deformation mechanism of the tubes is progressive and efficient, maintaining a balance between structural stiffness and energy dissipation capability. Such characteristics are desirable for crashworthiness applications, as they enable the structure to perform effectively under both low- and high-impact conditions.

The Mean Force (MF) value plays an important role in determining

Table 1
Crashworthiness performance.

Speciment	Mass (Kg)	Ea (kJ)	SEA (kJ/Kg)	IPFC (kN)	MF (kN)	CFE (%)
HPVS	0.16	2.844	17.77	47.156	58.45	1.23
HPSR	0.16	3.522	22.01	56.763	56.71	0.99
HPMR	0.161	3.067	19.05	46.938	56.11	1.19
HPLR	0.161	3.050	18.94	46.613	58.24	1.24

the stability and efficiency of energy absorption during the axial deformation process. A high MF value indicates the ability of the structure to maintain a relatively constant compressive force after the initial peak phase (Initial Peak Force), reflecting a high energy absorption capacity and resistance to deformation without significant loss of structural stability. This condition is highly advantageous for energy-absorbing applications under high-impact conditions, such as vehicle safety zones, where the structure must effectively dissipate energy throughout the crushing process. However, an excessively high MF may increase the transmitted force to the surrounding structure or passengers, potentially reducing comfort and increasing the risk of injury [41, 35]. Conversely, a low MF value indicates a reduction in structural stiffness after the peak phase, which suggests a decreased ability to absorb energy per unit deformation and may lead to non-uniform deformation (buckling) or premature structural collapse. Therefore, an ideal MF value should balance deformation stability and energy absorption capacity by maintaining a sufficiently high but progressive average force to ensure optimal crashworthiness performance [4].

As shown in Table 1, the crashworthiness performance characteristics of the developed hybrid tube designs demonstrate a close relationship between structural mass and Mean Force (MF). An increase in structural mass directly influences the energy absorption capacity as well as the stability of the compressive force during the axial deformation process. In this study, the four specimens have relatively similar masses, ranging from 0.160–0.161 kg, yet they still exhibit variations in MF values between 56–58 kN. This phenomenon indicates that the differences in crashworthiness performance are more strongly influenced by the internal geometric configuration than by the total structural mass. From a theoretical perspective, a larger mass tends to increase structural inertia and the ability of the structure to withstand axial loading, resulting in higher MF values because the structure can maintain a constant compressive force over a longer deformation range [41]. However, excessive mass may reduce the efficiency of specific energy absorption (SEA), since the absorbed energy does not increase proportionally with the total structural weight [35]. Conversely, an excessively low mass may lead to a reduction in MF due to decreased stiffness and structural inertia, which may ultimately increase the risk of non-uniform deformation or premature buckling. Therefore, the optimal structural mass should achieve a balance being sufficiently large to maintain a high and stable mean force, while remaining lightweight to preserve energy absorption efficiency per unit mass. These findings highlight that the relationship among mass, geometric configuration, and material stiffness is a critical factor in optimizing hybrid tube structures for crashworthiness applications in the automotive and aerospace industries [37].

Based on Fig. 7a, which presents the comparison of Specific Energy Absorption (SEA) and Crush Force Efficiency (CFE), the four specimens (HPVS, HPSR, HPMR, and HPLR) exhibit significant differences in both parameters. The SEA value for HPSR (22.01 kJ/Kg) is the highest, followed by HPMR (19.05 kJ/Kg), HPLR (18.94 kJ/Kg), and HPVS (17.77 kJ/Kg). This result indicates that the HPSR configuration has the greatest energy absorption capacity among all specimens, which is consistent with the observed increase in Energy Absorption (EA) and the optimal stability of its deformation behavior. The higher SEA value suggests that the HPSR structure is capable of optimizing structural deformation during axial crushing, allowing the structure to absorb more energy through controlled deformation mechanisms [41]. These findings are further confirmed in Fig. 7b, which shows the SEA–CFE curve describing the relationship between SEA and CFE for each specimen. The points on the curve indicate that HPSR combines a high SEA value with a relatively lower CFE. This suggests that although HPSR is highly efficient in absorbing energy, noticeable force fluctuations occur during the crushing process, resulting in an imbalance between the peak force and the mean force. Consequently, while HPSR is more efficient in absorbing energy under quasi static conditions, this configuration may be less effective for low- to medium-impact scenarios where a more stable force distribution is required [2,42]. In contrast, the HPLR model exhibits the highest CFE value. This indicates that although its SEA value is lower than that of HPSR, HPLR provides a more stable force distribution throughout the crushing process. Structures with higher CFE values are more effective at distributing compressive forces, thereby reducing the likelihood of injury or damage to connected structural components. Therefore, the HPLR configuration is more suitable for applications involving low- to medium-impact loads, where force stability and deformation control are more critical than achieving extremely high energy absorption capacity.

The highest Crush Force Efficiency (CFE) values were recorded for HPLR (1.24) and HPVS (1.23), followed by HPMR (1.19) and HPSR (0.99). The relatively lower CFE value observed in the HPSR configuration indicates that although the peak force is high, a significant reduction in load occurs as the structure transitions to the mean-force deformation phase. This behavior suggests a more stable progressive deformation mechanism characterized by controlled folding (concertina fold). This phenomenon supports the theory proposed by Gowid et al. [4], which explains that the combination of hybrid metal–composite materials can produce a layered deformation mechanism with gradually dissipated energy phases, allowing the structure to absorb more energy without losing structural stability. The ideal CFE value is approximately 1, indicating that the ratio between the average crushing force (F_{avg}) and the global peak crushing force (G_{PCF}) is nearly equal. Under such conditions, the force–displacement curve tends to remain relatively steady

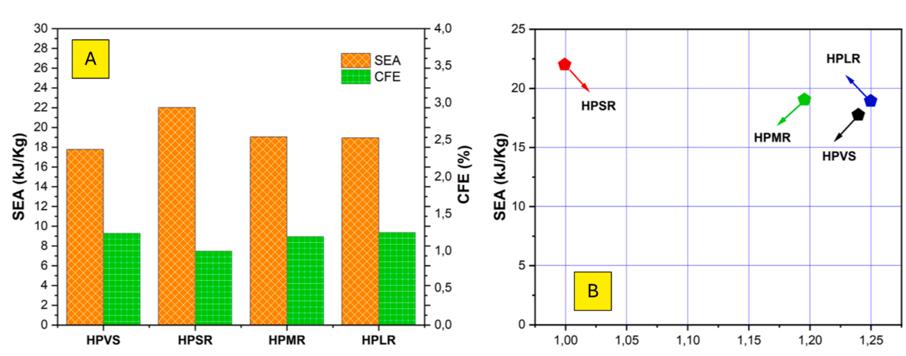

Fig. 7. (a) Comparison of SEA and CFE (b) distribution of hybrid tube configurations on the SEA–CFE plot.

Table 2
Comparison of the crashworthiness of different sections.

Design Tubes	m (kg)	t (mm)	EA (kJ)	SEA (kJ/Kg)	CFE (%)	PFC (kN)	Reference
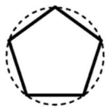	0.259	2.04	3.446	13.31	0.440	65.24	[21]
	0.127	1.00	1.181	9.30	0.335	29.30	
	0.105	1.00	1.189	11.32	0.279	38.11	[23]
	0.259	1.10	2.709	10.46	0.378	59.74	[21]
	0.235	1.00	2.313	9.84	0.358	53.57	
	0.188	1.00	2.845	15.13	0.427	59.44	[23]
	1.110	2.00	19.455	17.52	49.82	187.69	[50]
	0.259	0.78	4.467	17.25	0.613	60.69	[21]
	0.332	1.00	6.321	19.01	0.629	83.30	
	0.259	0.53	4.980	19.23	0.717	57.88	[21]
	0.491	1.00	12.491	25.44	0.805	128.89	
	0.215	1.00	5.426	25.270	0.666	72.72	[23]
	0.266	1.00	8.587	32.280	0.794	98.503	[23]
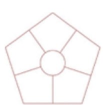	0.101	1.00	2.091	20.69	57.14	45.75	[24]
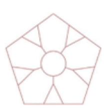	0.125	1.00	3.354	26.80	68.85	60.90	[24]
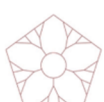	0.155	1.00	5.073	32.72	75.88	83.58	[24]
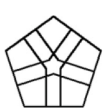	1.487	2.00	36.860	24.78	67.95	260.03	[50]
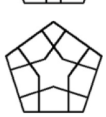	1.434	2.00	35.922	25.04	70.27	240.00	[50]
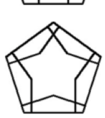	1.328	2.00	35.377	26.64	70.14	240.23	[50]
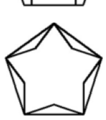	1.448	2.00	31.180	21.52	57.18	259.68	[50]

with stable peak fluctuations. Overall, the results of this analysis reveal a trade-off between energy absorption capacity and force distribution efficiency. The HPSR configuration, with the highest SEA value, is highly effective in absorbing energy under quasi static conditions. In contrast, the HPLR configuration demonstrates superior force distribution efficiency, making it more suitable for applications involving low-energy impacts. These findings provide important insights for the design of crashworthiness protection components, particularly in vehicles and other protective structures, where achieving a balance between energy absorption capacity and force distribution is crucial for safety and optimal structural performance.

Table 2 shows that the crashworthiness performance of thin-walled tubes is simultaneously influenced by several factors, including the cross-sectional shape, hierarchical topology, internal cell configuration, thickness distribution, and the deformation mechanisms that develop during axial loading. In general, the comparative data presented in the table reveal a consistent trend indicating that the implementation of hierarchical or fractal structures enhances energy absorption capacity compared with conventional configurations. Hierarchical structures are capable of forming more stable progressive folding patterns, increasing

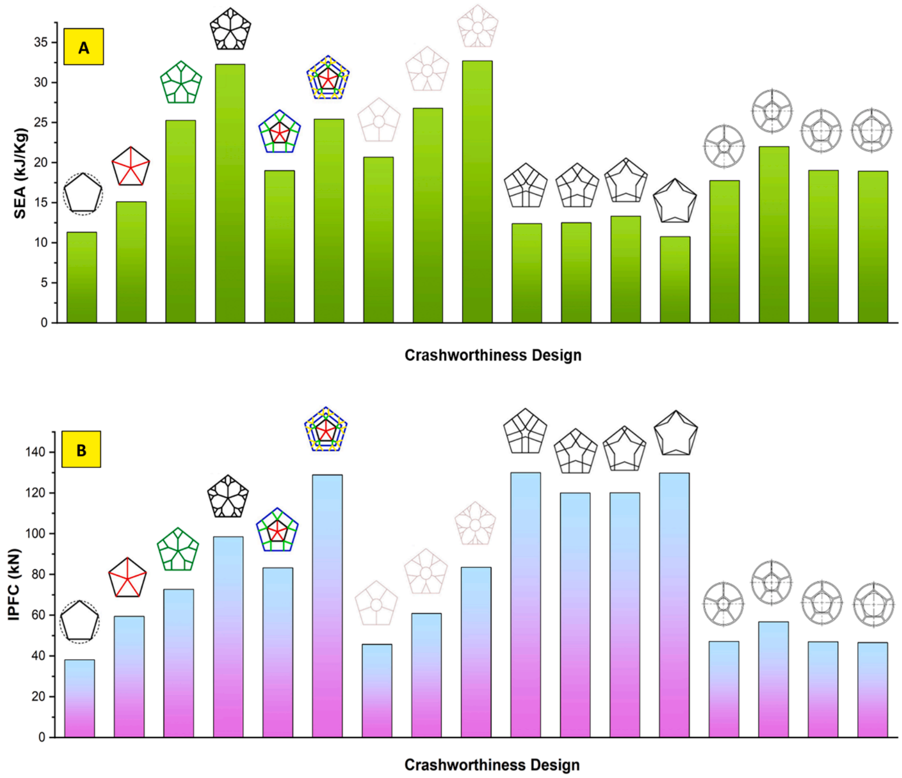

Fig. 8. Crashworthiness performance of pentagonal designs (a) SEA and (b) IPFC.

the number of plastic hinges and improving force distribution during the crushing process [21,23,24]. Therefore, improvements in crashworthiness performance are not solely determined by changes in cross-sectional geometry but are primarily influenced by the effectiveness of the internal structural architecture in controlling the initiation and propagation of folding mechanisms. A similar phenomenon was observed in the HPSR configuration in this study, where a well-controlled deformation pattern resulted in enhanced stability and maximum energy absorption capacity.

For tree-like fractal hierarchical multicellular pentagonal tubes, increasing the hierarchical order generally leads to improved crashworthiness performance, as summarized in Table 2. Specifically, the addition of hierarchical branches not only increases the energy absorption capacity but also results in a higher Initial Peak Crushing Force (IPFC) [23]. A high IPFC is considered unfavorable because, during the initial stage of impact, the structure tends to transmit a large peak force to the protected system. Consequently, the force transferred to passengers or primary structural components becomes greater. In this regard, the hybrid tube design provides a more balanced combination of EA, SEA, CFE, and PFC, as illustrated in Fig. 8. The pentagonal hybrid tube design exhibits superior deformation stability due to the increased number of folds and the reduced half-wavelength of the folding pattern. These findings suggest that improved crashworthiness performance in hierarchical structures is reflected not only by increased SEA values but also by lower IPFC values. The HPSR configuration, which achieved the highest EA and SEA among all pentagonal variations, indicates that proper control of internal pentagonal spacing can provide an optimal compromise among energy absorption capacity, progressive deformation stability, and peak load control.

3.3. Final deformation in crashworthiness analysis

Fig. 9. presents the final deformation profiles of the four pentagonal multi-cell hybrid tube models after axial loading. Each model exhibits a different deformation pattern, indicating variations in structural stability, folding behavior, and energy dissipation efficiency during the crushing process. Overall, three main deformation modes are identified in all models, namely concertina, diamond, and buckling, each of which contributes differently to the overall crashworthiness performance.

The HPSR model exhibits a concertina folding pattern that develops uniformly and symmetrically along the deformation axis. This mode indicates a stable progressive folding mechanism, in which impact energy is absorbed efficiently through the formation of evenly distributed plastic hinges at each stage of deformation. The hybrid material located on the inner side helps prevent premature local buckling of the aluminum tube. The failure mechanism is likely initiated at the edges of the pentagonal cells, followed by gradual plastic deformation as energy is efficiently dissipated by the material. As a result, the structure undergoes symmetric deformation, and the fracture mechanism is dominated by controlled folding. This deformation pattern is consistent with the high Specific Energy Absorption (SEA) and moderate Crush Force Efficiency (CFE) values, indicating an optimal balance between structural stiffness and controlled deformation. The concertina deformation mode is particularly desirable because it maintains load stability and maximizes impact energy absorption through uniform material folding rather than localized cracking [38].

In contrast, the HPLR model exhibits a combination of concertina deformation and slight buckling in the midsection of the tube, indicating partial instability during the crushing process. This configuration is expected to produce larger and more irregular folds due to the substantial diameter difference between the internal and external cells. Buckling failure is likely to initiate earlier than in the HPSR model, as the larger cell size promotes asymmetric deformation. Local cracking and buckling tend to occur in the upper region of the structure, thereby reducing energy absorption efficiency during the initial stage of crushing. The fracture mechanism of this model is primarily governed by local instability and crack propagation, especially under higher loading conditions. This deformation behavior leads to a slightly lower SEA value but a higher CFE value, suggesting a more uniform force distribution despite the reduced energy absorption capacity. By comparison, the

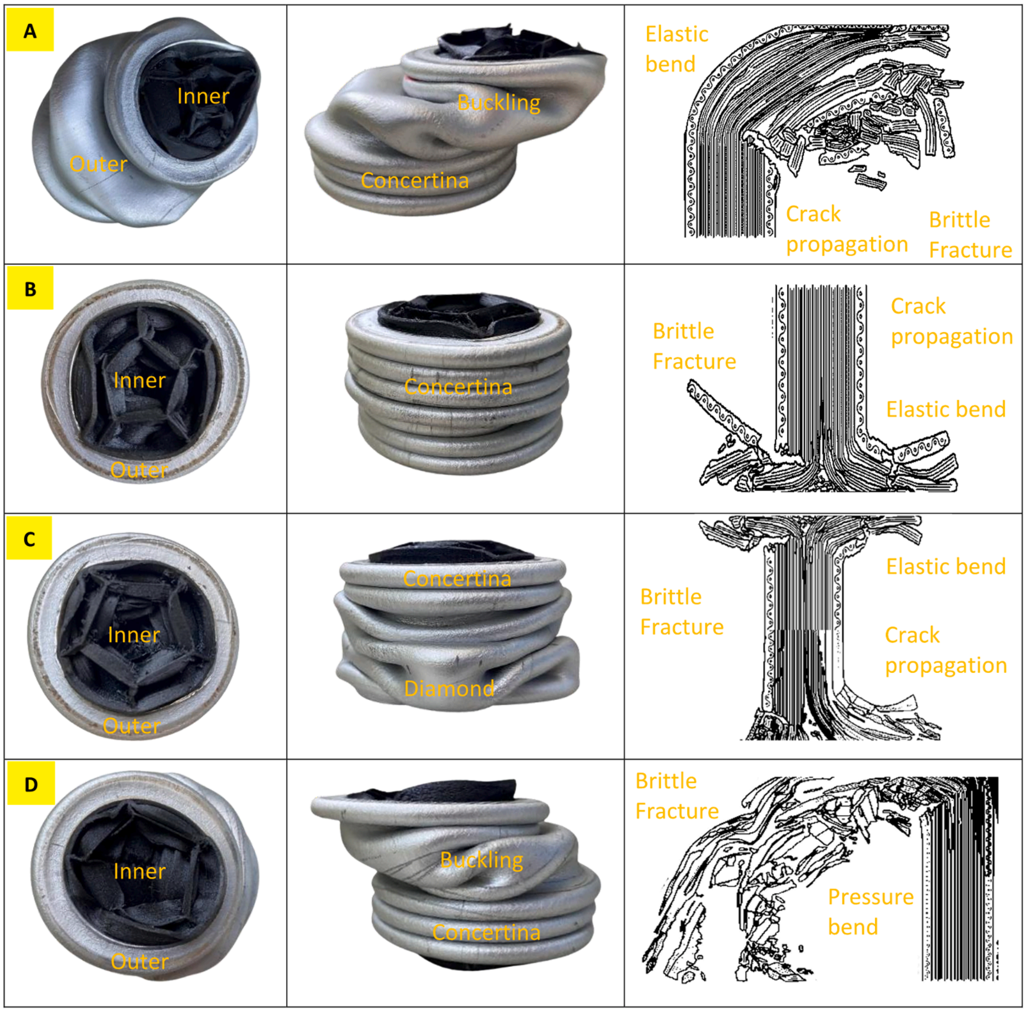

Fig. 9. Final deformation and failure characteristics of pentagonal hybrid tube.

greater stiffness associated with the geometric configuration of the HPSR model tends to generate a more uniform force response due to the delayed onset of local buckling [43–47].

The HPMR model exhibits a mixed deformation mechanism, initially characterized by concertina folding and subsequently transitioning into diamond folds during the final stage of deformation. This behavior indicates a moderate energy dissipation capacity accompanied by partial structural stability. The failure mechanism may begin with early local buckling in the upper and lower regions of the internal cells, followed by the development of diamond-shaped folds in localized areas. Cracks are likely to initiate at the corners of the pentagonal cells; however, the resulting fold formation still permits a considerable amount of energy to be dissipated. The occurrence of diamond folds is generally associated with irregular axial load paths or loading conditions that are not fully symmetric. Nevertheless, the progressively formed folds in the HPMR model still allow the structure to maintain relatively favorable SEA and CFE values [37,48,49].

In the HPVS model, early buckling is observed in the upper region of the tube, followed by the formation of irregular folds in the lower section, indicating a less stable deformation mode dominated by local bending and twisting. This behavior reduces the efficiency of energy absorption. The early buckling in the HPVS configuration is likely associated with the smaller diameter of the internal cells, which causes high stress concentrations at specific points, thereby triggering local instability and promoting crack initiation along the edges of the pentagonal cells. This deformation pattern is characterized by irregular folding and the potential occurrence of local fracture, leading to inefficient energy absorption and non-uniform structural failure. Buckling and local cracking that develop during the early stage of deformation may significantly reduce the energy dissipation capacity of the structure [6,50].

4. Conclusion

This study investigated the effect of internal diameter variation in pentagonal multi-cell carbon filament/aluminum circular hybrid tubes on crashworthiness performance under quasi-static axial loading. The findings demonstrate that the HPSR configuration achieved the best overall performance, with an EA of 3.522 kJ, an SEA of 22.01 kJ/kg, and an IPF of 56.76 kN, indicating the highest energy absorption capacity among all specimens. By comparison, the HPMR, HPLR, and HPVS configurations yielded lower EA values of 3.067 kJ, 3.050 kJ, and 2.844 kJ, respectively. In terms of deformation behavior, the HPSR model exhibited a stable and progressive concertina folding mode, whereas the HPVS model experienced early buckling and the HPLR model displayed local instability, despite achieving the highest CFE value of 1.24. Overall, the small-range pentagonal configuration can be regarded as the most optimal design, as it provides a well-balanced combination of EA, SEA, CFE, and PFC for future energy-absorbing applications. In addition, the integration of hybrid materials within fractal hierarchical multicellular designs offers promising potential for further enhancing EA performance.

CRediT authorship contribution statement

Willy Artha Wirawan: Conceptualization, Funding acquisition, Investigation, Methodology, Supervision, Validation, Writing – original draft, Writing – review & editing. **Delia Hani Wakhidah:** Investigation, Project administration, Resources, Software, Validation, Visualization, Writing – review & editing. **Diah Wulandari:** Data curation, Formal analysis, Project administration, Resources, Software. **A'yan Sabitah:** Data curation, Investigation, Methodology, Project administration, Resources, Visualization. **Moch. Agus Choiron:** Supervision, Validation, Writing – review & editing. **Joewono Prasetijo:** Supervision, Validation, Writing – review & editing. **S.M. Sapuan:** Supervision, Validation, Writing – review & editing.

Declaration of competing interest

The authors declare that they have no known competing financial interests or personal relationships that could have appeared to influence the work reported in this paper.

Acknowledgment

The authors gratefully acknowledge the financial support of the Program Penelitian Kompetitif RKI-2026, Institute for Research and Community Service (LPPM), Universitas Negeri Surabaya. The authors also express their sincere appreciation to the Faculty of Vocational and Technical Studies, Universitas Negeri Surabaya, for providing laboratory facilities and technical assistance. The authors further thank Politeknik Negeri Banjarmasin, Universitas Brawijaya, Universiti Tun Hussein Onn Malaysia, and Universiti Putra Malaysia for their valuable collaboration and academic support, which significantly contributed to this study.

Data availability

Data will be made available on request.

References

[1] S. Widi Astuti, W. Artha Wirawan, A. Zulkarnain, D. Tri Istiantara, Comparison of energy absorption and pattern of deformation material crash box of three segments with Bilinear and Johnson Cook approach, J. Phys.: Conferenc. Seri. 1273 (1) (2019), https://doi.org/10.1088/1742-6596/1273/1/012078.

[2] G. Zhu, G. Sun, H. Yu, S. Li, Q. Li, Energy absorption of metal, composite and metal/composite hybrid structures under oblique crushing loading, Int. J. Mech. Sci. 135 (2018) 458–483, https://doi.org/10.1016/j.ijmecsci.2017.11.017.

[3] C. Reuter, T. Tröster, Crashworthiness and numerical simulation of hybrid aluminium-CFRP tubes under axial impact, Thin-Walled Structure. 117 (2017) 1–9, https://doi.org/10.1016/j.tws.2017.03.034.

[4] S. Gowid, E. Mahdi, J. Renno, S. Sassi, G. Kharmanda, A. Shokry, Experimental investigation of the crashworthiness performance of fiber and fiber steel-reinforced composites tubes, Compos. Struct. (2020) 251, https://doi.org/10.1016/j.compstruct.2020.112655.

[5] M.M. Awd Allah, M.A. Abd El-baky, Multi-objective optimization through desirability function analysis on the crashworthiness performance of thermoplastic/thermoset hybrid structures, Compos. Part B: Eng. 284 (July) (2024) 111742, https://doi.org/10.1016/j.compositesb.2024.111742.

[6] W.A. Wirawan, A. Choiron Moch, H.B. Wahjono, F. Rozaq, N.F. Rachman, M. J. Alfana, Experimental quasi-static test for the energy absorber tube in high-speed train (HST), in: Proceedings of the International Conference on Railway and Transportation (ICORT 2022) (Vol. 1), Atlantis Press International BV, 2023, https://doi.org/10.2991/978-94-6463-126-5.

[7] R. Jiang, Z. Gu, T. Zhang, D. Liu, H. Sun, Z. Pan, D. Peng, Energy absorption characteristics of a cfrp-al hybrid thin-walled circular tube under axial crushing, Aerospace 8 (10) (2021), https://doi.org/10.3390/aerospace8100279.

[8] S. Ming, Z. Song, C. Zhou, K. Du, C. Teng, Y. Wang, S. Xu, B. Wang, The crashworthiness design of metal /CFRP hybrid tubes based on origami-ending approach : experimental research, Compos. Struct. 279 (2022) 114843, https://doi.org/10.1016/j.compstruct.2021.114843.

[9] D. Le, N. Novak, A. Arjunan, A. Baroutaji, Q. Estrada, Thin-walled structures crashworthiness of bio-inspired multi-stage nested multi-cell structures with foam core, Thin-Walled Structure. 182 (2023) 110245, https://doi.org/10.1016/j.tws.2022.110245.

[10] G. Luo, J. Liu, L. Li, P. Xue, J. Zhao, Y. Chen, International Journal of Mechanical Sciences Crashworthiness analysis and multi-objective optimization design for foam-filled spiral tube, Int. J. Mech. Sci. 282 (2024) 109588, https://doi.org/10.1016/j.ijmecsci.2024.109588.

[11] Y. Xiong, H. Yang, X. Li, H. Lei, G. Lu, Heliyon Crashworthy optimization of skeleton-filled FRP tubes based on back propagation neural network, Heliyon. 9 (12) (2023) e23019, https://doi.org/10.1016/j.heliyon.2023.e23019.

[12] J. Bidadi, M. Arabha, H.S. Googarchin, International journal of adhesion and adhesives bonding in automotive hybrid multi-cell square tubes : experimental and numerical investigation on quasi-static axial crashworthiness performance, Int. J. Adhesion Adhesives 135 (2024) 103832, https://doi.org/10.1016/j.ijadhadh.2024.103832.

[13] X. Fu, X. Zhang, Z. Huang, Axial crushing of nylon and Al/Nylon hybrid tubes by FDM 3D printing, Compos. Struct. 256 (2021) 113055, https://doi.org/10.1016/j.compstruct.2020.113055.

[14] R. Yao, T. Pang, B. Zhang, J. Fang, Q. Li, G. Sun, On the crashworthiness of thin-walled multi-cell structures and materials: state of the art and prospects, Thin-Walled Structure. 189 (2023) 110734, https://doi.org/10.1016/j.tws.2023.110734.

[15] A.D. Nugraha, R.K. Adi, V.V. Kumar, A. Kusumawanto, B. Prawara, E. Junianto, M. F. Hikmawan, M.A. Muflikhun, Investigating the mechanical properties and crashworthiness of hybrid PLA/GFRP composites fabricated using FDM-filament winding, Heliyon. 10 (20) (2024), https://doi.org/10.1016/j.heliyon.2024.e39062.

[16] Z. Jiang, J. Zhao, W. Chen, H. Lv, Experimental and numerical crashworthiness investigation of 3D printing carbon fiber reinforced nylon origami tubes, Polym. Compos. 45 (4) (2024) 3296–3314, https://doi.org/10.1002/PC.27991.

[17] M. Tunay, C.U. Deniz, D. Kazel, Experimental investigation on crashworthiness behaviors of 3D-printed cellular composite sandwich structures, Polym. Compos. 46 (15) (2025) 14433–14446, https://doi.org/10.1002/PC.30071.

[18] Z. Cai, X. Deng, Recent advances in reinforced honeycomb mechanical metamaterials: a review, Mater. Des. 263 (2026) 115593, https://doi.org/10.1016/J.MATDES.2026.115593.

[19] Z. Cai, X. Deng, Energy absorption characteristics of novel hybrid honeycombs under axial crushing, Archive. Civil Mech. Eng. 25 (4) (2025) 1–27, https://doi.org/10.1007/s43452-025-01286-4.

[20] S. Xu, Q. Fu, X. Guang, H. Huang, X. Deng, Performance study of two-ways gradient octagonal hierarchical honeycomb with excellent energy absorption and crashworthiness properties, J. Ind. Inf. Integr. 47 (2025) 100925, https://doi.org/10.1016/j.jii.2025.100925.

[21] X. Deng, G. Wang, Z. Cai, Crashworthiness of multicellular tubes with tree-like fractal hierarchical structure under axial impact, Mech. Adv. Mater. Structure. 31 (28) (2024) 10081–10097, https://doi.org/10.1080/15376494.2023.2284430.

[22] X. Deng, Y. Chen, J. Huang, Crashworthiness analysis of hexagonal hierarchical gradient tubes with axial variable thickness inspired by tree fractal structure, Mech. Adv. Mater. Structure. 31 (21) (2024) 5398–5413, https://doi.org/10.1080/15376494.2023.2215778.

[23] J. Wu, Y. Zhang, F. Zhang, Y. Hou, X. Yan, A bionic tree-liked fractal structure as energy absorber under axial loading, Eng. Struct. 245 (2021) 112914, https://doi.org/10.1016/j.engstruct.2021.112914.

[24] Z. Guo, J. Hu, Z. Kong, On the crashworthiness of bionic fractal multi-cell tubes under axial and oblique loadings – Numerical study, theoretical predication and optimization, Structures 78 (2025) 109355, https://doi.org/10.1016/j.istruc.2025.109355.

[25] R.A. Eshkoor, S.A. Oshkovr, A.B. Sulong, R. Zulkifli, A.K. Ariffin, C.H. Azhari, Effect of trigger configuration on the crashworthiness characteristics of natural silk epoxy composite tubes, Compos. Part B: Eng. 55 (1) (2013) 5–10, https://doi.org/10.1016/j.compositesb.2013.05.022.

[26] M.F.M. Alkbir, S.M. Sapuan, A.A. Nuraini, M.R. Ishak, Fibre properties and crashworthiness parameters of natural fibre-reinforced composite structure: a literature review, Compos. Struct. 148 (2016) 59–73, https://doi.org/10.1016/j.compstruct.2016.01.098.

[27] S.N. Fitriah, M.S. Abdul Majid, M.J.M. Ridzuan, R. Daud, A.G. Gibson, T. A. Assaleh, Influence of hydrothermal ageing on the compressive behaviour of glass fibre/epoxy composite pipes, Compos. Struct. 159 (2017) 350–360, https://doi.org/10.1016/j.compstruct.2016.09.078.

[28] W. Artha Wirawan, A. Zulkarnain, H. Boedi Wahjono, A. Jamaludin Tyas Damayanti, The effect of material exposure variations on energy absorption capability and pattern of deformation material of crash box of three segments, J. Phys.: Conferenc. Seri. 1273 (1) (2019), https://doi.org/10.1088/1742-6596/1273/1/012081.

[29] W.A. Wirawan, B. Junipitoyo, S.H.S. Putro, A. Sabitah, A.H. Suudy, R. Ridwan, M. A. Choiron, Collapse behavior and energy absorption characteristics of design multi-cell thin wall structure 3D-printed under quasi statistic loads, Automotive Experienc. 7 (1) (2024) 149–160, https://doi.org/10.31603/ae.10892.

[30] S. Xie, P. Chen, N. Wang, J. Wang, X. Du, Crashworthiness study of circular tubes subjected to radial extrusion under quasi-static loading, Int. J. Mech. Sci. 192 (2021) 106128, https://doi.org/10.1016/j.ijmecsci.2020.106128.

[31] E.S. Yeshanew, G.M.S. Ahmed, D.K. Sinha, I.A. Badruddin, S. Kamangar, I. M. Alarifi, H.M. Hadidi, Experimental investigation and crashworthiness analysis of 3D printed carbon PA automobile bumper to improve energy absorption by using LS-DYNA, Adv. Mech. Eng. 15 (6) (2023) 1–23, https://doi.org/10.1177/16878132231181058.

[32] C. William, C. Ezekwem, A review of the crashworthiness performance of energy absorbing composite structure within the context of materials, manufacturing and

maintenance for sustainability, Compos. Struct. 257 (2021) 113081, https://doi.org/10.1016/j.compstruct.2020.113081.
[33] I. Choirotin, M.A. Choiron, A. Purnowidodo, D.B. Darmadi, Crashworthiness analysis and optimization of bi-tubular corrugated thin-walled tube under axial loading, Mech. Adv. Mater. Structur. 0 (0) (2025) 1–14, https://doi.org/10.1080/15376494.2025.2556266.
[34] S.E. Alkhatib, F. Tarlochan, A. Hashem, S. Sassi, Collapse behavior of thin-walled corrugated tapered tubes under oblique impact, in: Thin-Walled Structur., 122, 2018, pp. 510–528, https://doi.org/10.1016/j.tws.2017.10.044.
[35] W.A. Wirawan, A. Sabitah, G. Sakti, B.B. Harianto, M. Agus Choiron, R.A. Ilyas, S. M. Sapuan, J. Prasetijo, Crashworthiness characteristic of aluminum/composite hybrid tubes under axial compression, Results. Eng. 25 (2025) 103889, https://doi.org/10.1016/j.rineng.2024.103889.
[36] D.H. Wakhidah, M.A. Choiron, Y.S. Irawan, A. Purnowidodo, Energy absorption and deformation pattern of circular hybrid crash box subjected to frontal load, MM Sci. J. (2024) 7222–7229, https://doi.org/10.17973/MMSJ.2024_02_2023094.
[37] X. Jia, G. Chen, Y. Yu, G. Li, J. Zhu, X. Luo, C. Duan, X. Yang, D. Hui, Effect of geometric factor, winding angle and pre-crack angle on quasi-static crushing behavior of filament wound CFRP cylinder, Compos. Part B: Eng. 45 (1) (2013) 1336–1343, https://doi.org/10.1016/j.compositesb.2012.09.060.
[38] Z. Zhang, C. Guo, L. Wang, D. Hu, Crashworthiness of bio-inspired hierarchical hybrid multi-cell tubes under axial crushing, Eng. Fail. Anal. 166 (2024) 108886, https://doi.org/10.1016/j.engfailanal.2024.108886.
[39] K. Feng, G. Wei, H. Yu, L. Yao, W. Wang, Y. Shen, X. Yan, Y. Ma, Effect of geometric structure and fiber orientation on crashworthiness of honeycomb-inspired composite thin-walled tubes, Polym. Compos. 45 (10) (2024) 9600–9619, https://doi.org/10.1002/PC.28430.
[40] W. Shun, M. Qi-hua, G. Xue-hui, Z. Tian-jun, Crashworthiness analysis and multi-objective optimization of Al/CFRP tubes with induced holes, Polym. Compos. 42 (10) (2021) 5280–5299, https://doi.org/10.1002/PC.26222.
[41] M. Zang, Y. Hu, J. Zhang, W. Ye, M. Zhao, Crashworthiness of CFRP/aluminum alloy hybrid tubes under quasi-static axial crushing, J. Mater. Res. Technol. 9 (4) (2020) 7740–7753, https://doi.org/10.1016/j.jmrt.2020.05.046.
[42] H. Liang, B. Liu, Y. Pu, H. Sun, D. Wang, Crashworthiness analysis of variable thickness CFRP/Al hybrid multi-cell tube, Int. J. Mech. Sci. 266 (2024) 108959, https://doi.org/10.1016/j.ijmecsci.2024.108959.
[43] W. Cai, Q. Ma, Y. Wang, X. Gan, Crashworthiness analysis and multi-objective optimization of Al/CFRP hybrid tube with initial damage under transverse impact, Polym. Compos. 44 (11) (2023) 7953–7971, https://doi.org/10.1002/PC.27678.
[44] Y. Ma, H. Huang, X. Deng, Research on the in-plane energy absorption characteristics of the novel rotating self-similar star-shaped honeycomb structure, Eng. Fail. Anal. 189 (2026) 110696, https://doi.org/10.1016/J.ENGFAILANAL.2026.110696.
[45] S. Mudassir, M. Vinayaka Kulkarni, S. Sivamani, Modelling and fabrication of synthetic-natural fibre sandwich structure for fish feeder hull, in: Materials Today: Proceedings, 2023, https://doi.org/10.1016/J.MATPR.2023.02.141.
[46] N. Qiu, Z. Yu, D. Wang, M. Xiao, Y. Zhang, N.H. Kim, J. Fang, Bayesian optimization of origami multi-cell tubes for energy absorption considering mixed categorical-continuous variables, Thin-Walled Structur. 199 (2024) 111799, https://doi.org/10.1016/j.tws.2024.111799.
[47] D.H. Wakhidah, M.A. Choiron, A. Purnowidodo, Y.S. Irawan, Crashworthiness performance of circular hybrid crash box due to axial load, Int. J. Integrat. Eng. 16 (2) (2024) 182–194, https://doi.org/10.30880/ijie.2024.16.02.019.
[48] H. Yulong, J. Tao, L. Xin, Q. Ji, S. Xuefeng, Crashworthiness design of hexagonal tubes using self-similar inspired structures, Mater. Today Commun. 33 (October) (2022) 104934, https://doi.org/10.1016/j.mtcomm.2022.104934.
[49] L. Zhang, Z. Bai, F. Bai, Thin-Walled Structures crashworthiness design for bio-inspired multi-cell tubes with quadrilateral, hexagonal and octagonal sections, Thin Walled Structur. 122 (2018) 42–51, https://doi.org/10.1016/j.tws.2017.10.010.
[50] Z. Ghahremanzadeh, S. Pirmohammad, Crashworthiness performance of square, pentagonal, and hexagonal thin-walled structures with a new sectional design, Mech. Adv. Mater. Structur. 30 (12) (2023) 2353–2370, https://doi.org/10.1080/15376494.2022.2053910.